Cellular/Molecular

CLHM-1 is a Functionally Conserved and Conditionally Toxic Ca^{2+}-Permeable Ion Channel in *Caenorhabditis elegans*

Jessica E. Tanis, Zhongming Ma, Predrag Krajacic, Liping He, J. Kevin Foskett, and Todd Lamitina
Department of Physiology, Perelman School of Medicine, University of Pennsylvania, Philadelphia, Pennsylvania 19104

Disruption of neuronal Ca^{2+} homeostasis contributes to neurodegenerative diseases through mechanisms that are not fully understood. A polymorphism in CALHM1, a recently described ion channel that regulates intracellular Ca^{2+} levels, is a possible risk factor for late-onset Alzheimer's disease. Since there are six potentially redundant CALHM family members in humans, the physiological and pathophysiological consequences of CALHM1 function *in vivo* remain unclear. The nematode *Caenorhabditis elegans* expresses a single CALHM1 homolog, CLHM-1. Here we find that CLHM-1 is expressed at the plasma membrane of sensory neurons and muscles. Like human CALHM1, *C. elegans* CLHM-1 is a Ca^{2+}-permeable ion channel regulated by voltage and extracellular Ca^{2+}. Loss of *clhm-1* in the body-wall muscles disrupts locomotory kinematics and biomechanics, demonstrating that CLHM-1 has a physiologically significant role *in vivo*. The motility defects observed in *clhm-1* mutant animals can be rescued by muscle-specific expression of either *C. elegans* CLHM-1 or human CALHM1, suggesting that the function of these proteins is conserved *in vivo*. Overexpression of either *C. elegans* CLHM-1 or human CALHM1 in neurons is toxic, causing degeneration through a necrotic-like mechanism that is partially Ca^{2+} dependent. Our data show that CLHM-1 is a functionally conserved ion channel that plays an important but potentially toxic role in excitable cell function.

Introduction

Ca^{2+} acts as an intracellular messenger required for essential processes including neurotransmitter release and muscle contraction. Multiple active and passive mechanisms are used to precisely regulate cytoplasmic Ca^{2+} including Ca^{2+} pumps and cotransporters, voltage-gated Ca^{2+} channels (VGCCs), transient receptor potential (TRP) channels, store-operated Ca^{2+} entry (SOCE) channels, hemichannels, inositol 1,4,5-triphosphate ($InsP_3$) receptors, and ryanodine receptors (Berridge et al., 1998). Disruption of neuronal Ca^{2+} homeostasis, either through inappropriate entry of extracellular Ca^{2+} (Ca_o^{2+}) or unregulated release of Ca^{2+} from intracellular stores, has been linked to neurodegenerative diseases such as Alzheimer's disease (AD) (Bezprozvanny and Mattson, 2008). However, the molecular mechanisms that underlie alterations in cellular Ca^{2+} handling and AD pathogenesis are poorly understood.

Received Dec. 30, 2012; revised June 5, 2013; accepted June 7, 2013.

Author contributions: J.E.T., Z.M., J.K.F., and T.L. designed research; J.E.T., P.K., and L.H. performed research; J.E.T., Z.M., and P.K. analyzed data; J.E.T., J.K.F., and T.L. wrote the paper.

This work was supported by National Institutes of Health Grant R21NS072775 (T.L., J.K.F.), a summer research grant from Mount Desert Island Biological Laboratory (T.L.), and NIH Fellowship F32AR060128 and an American Heart Association postdoctoral fellowship (J.E.T.). Some nematode strains used in this work were provided by the *Caenorhabditis* Genetics Center, which is funded by the NIH National Center for Research Resources. We also thank the National Bioresource Project for the *tm4071* allele, Monica Driscoll for clones, and Adam Siebert and Akiyuki Taruno for helpful discussions.

The authors declare no competing financial interests.

Correspondence should be addressed to Dr. Todd Lamitina, Department of Physiology, Richards Research Building A700, Perelman School of Medicine, University of Pennsylvania, Philadelphia, PA 19104. E-mail: lamitina@mail.med.upenn.edu.

DOI:10.1523/JNEUROSCI.5919-12.2013

 0270-6474/13/3312275-12$15.00/0

Human CALHM1 is a previously described pore-forming subunit of an ion channel that modulates cellular Ca^{2+} homeostasis (Dreses-Werringloer et al., 2008; Ma et al., 2012). Heterologous expression of CALHM1 in *Xenopus* oocytes and N2A cells gives rise to a voltage and Ca_o^{2+}-sensitive, outwardly rectifying, Ca^{2+}-permeable current (Ma et al., 2012). CALHM1 is predicted to contain four transmembrane (tm) domains and exhibits structural and functional similarities with connexins, pannexins, and innexins, but does not form gap junctions or exhibit significant sequence similarity with known ion channels (Siebert et al., 2013). Human genetic studies suggest that a polymorphism in CALHM1 [proline at residue 86 replaced by leucine (P86L)] may be associated with age of onset of late-onset Alzheimer's disease (LOAD) (Dreses-Werringloer et al., 2008; Boada et al., 2010; Lambert et al., 2010), although existing genetic data supporting a role for CALHM1 in LOAD pathogenesis remain controversial (Bertram et al., 2008; Beecham et al., 2009; Minster et al., 2009). While these genetic data indicate a potential role for mutant CALHM1 in disease, the role of CALHM1 in regulating Ca^{2+} homeostasis *in vivo* is unknown. Thus, it is essential to determine physiological and pathophysiological functions of normal and mutant CALHM1 in an *in vivo* system to understand the role of CALHM1 in neuronal Ca^{2+} homeostasis and its relationship to LOAD.

Calhm1 is one of six members in the *Calhm* gene family in humans. Both genetic redundancy and the fact that CALHM proteins form a multimeric structure complicate the study of mammalian CALHM1 *in vivo* (Dreses-Werringloer et al., 2008; Siebert et al., 2013). Thus, analysis of a *Calhm* homolog in a simpler organism might yield insights into CALHM1 function. While

Calhm1 homologs are absent in *Drosophila* and yeast, *Caenorhabditis elegans* expresses a single homolog, *clhm-1*. We found that *C. elegans* CLHM-1 is an ion channel that shares biophysical and pharmacological properties with human CALHM1. *C. elegans* CLHM-1 is expressed at the plasma membrane of excitable cells, is required in body-wall muscles for coordinated locomotion, and causes cell death when overexpressed. Furthermore, expression of either *C. elegans* CLHM-1 or human CALHM1 in body-wall muscles can rescue *C. elegans clhm-1* mutant motility defects, suggesting that these two proteins may play a similar role *in vivo*. Our work establishes *Calhm* family members as a new, evolutionarily conserved class of physiologically significant and potentially toxic ion channels.

Materials and Methods

Nematode culture. C. elegans hermaphrodites were grown at 20° under standard conditions unless noted otherwise. Double-mutant strains were constructed using standard genetic techniques (Brenner, 1974), and all genotypes were confirmed by PCR and/or sequencing. The wild-type strain was Bristol N2; mutants used were *clhm-1(tm4071)*, *clhm-1(ok3617)*, *cnx-1(ok2234)*, *crt-1(ok948)*, *mec-4(e1611)*, and *unc-119(ed3)*. Both *clhm-1* mutants were backcrossed four times to wild-type to remove background mutations.

Electrophysiology in Xenopus *oocytes*. The *C. elegans clhm-1* cDNA was inserted into the pBF oocyte expression vector; the CLHM-1 D125A mutation was created using the QuikChange II site-directed mutagenesis kit (Agilent Technologies). cRNA was synthesized from linearized plasmids with SP6 RNA polymerase (mMessage mMachine kit; Ambion). Five nanograms of *clhm-1* cRNA along with 80 ng of *Xenopus* connexin 38 (Cx38) antisense oligonucleotide (Ma et al., 2012) were injected into stage IV–VI *Xenopus* oocytes that had been isolated from female *Xenopus laevis* and defolliculated with type IV collagenase (Worthington Biochemical). Oocytes were incubated 1–3 d at 16°C in ND96 medium (96 mM NaCl, 2 mM KCl, 1.8 mM $CaCl_2$, 1 mM $MgCl_2$, 2.5 mM Na-pyruvate, 1× penicillin–streptomycin, pH 7.6). Oocytes injected with *clhm-1::gfp* cRNA were imaged with a Zeiss LSM 510 confocal microscope 48 h after injection.

Oocytes used for two-electrode voltage-clamp experiments were injected with 50 nl of a 20 mM BAPTA, 10 mM Ca^{2+} solution at least 30 min before recording to prevent activation of endogenous Ca^{2+}-activated Cl^- currents (Ma et al., 2012). Standard bath solutions contained 100 mM Na^+, 100 mM Cl^-, 2 mM K^+, and 10 mM HEPES, and various concentrations of Ca^{2+} and Mg^{2+} as indicated. EGTA (0.5 mM) and EDTA (0.5 mM) were added to the standard bath solution lacking divalent cations to create a divalent cation-free solution. All solutions were pH 7.2, adjusted with methanesulfonic acid. Data were acquired with an OC-725C amplifier (Warner Instrument) at 1 kHz with a 16 bit analog-to-digital converter (Instrutech ITC-16). Electrodes were made from thin-walled TW100F-6 glass (World Precision Instruments) using a micropipette puller (model P-87; Sutter Instrument) and were filled with 3 M KCl. All recordings were analyzed with Igor Pro.

Relative permeabilities. For ion permeability experiments, sucrose was used as substitute for NaCl or divalent cations in solutions to maintain constant osmolality while varying ion concentrations. KCl (3 M) agar bridges connected ground electrodes to bath solutions. Reversal potentials (E_{rev}) obtained from instantaneous *I–V* recordings were used in the Goldman–Hodgkin–Katz (GHK) constant field equation to estimate relative K^+, Na^+, and Cl^- permeabilities (Hille, 2001). Estimations of relative Ca^{2+} and Mg^{2+} permeabilities were calculated using the extended GHK equation (Jan and Jan, 1976; Ma et al., 2012).

Pharmacology. The standard bath solution for pharmacology experiments contained 100 mM Na^+, 100 mM Cl^-, and 10 mM HEPES in the presence or absence of 5 Ca^{2+}. Stock solutions of all potential inhibitors (Sigma-Aldrich) were made as follows: 200 mM MK801, 90 mM niflumic acid, 1.5 mM thapsigargin, and 120 mM nimodipine in DMSO; 450 mM 2-aminoethoxydiphenyl borate (2-APB) in MeOH; 770 mM octanol in EtOH; and 40 mM Ruthenium red, 50 mM SKF96365, 25 mM $ZnCl_2$, 100 mM $GdCl_3$, and 163 mM carbenoxolone in H_2O. Stock solutions were added to 0 mM Ca^{2+} pharmacology bath solution to final concentrations as indicated in Figure 2.

Sequence analysis. The multiple sequence alignment (Fig. 1) was created by the Clustal W method using MegAlign (Lasergene). The hypothetical model of *C. elegans* CLHM-1 was constructed using the transmembrane domain predictions from the TMPred (http://www.ch.embnet.org/software/TMPRED_form.html) and TMHMM (http://www.cbs.dtu.dk/services/TMHMM/) servers. The accession numbers of the sequences used were as follows: *C. elegans* CLHM-1, NP_495403; human CALHM1, NP_001001412.

Transgenes. The transgene used to examine the *clhm-1* expression pattern was generated by directly injecting a 3 kb *clhm-1* promoter::*gfp*::*unc-54* 3′ UTR PCR product (50 ng/μl) amplified from the plasmid pJT46 with pRol-6 (100 ng/μl) into wild-type animals, using the standard germline transformation technique (Mello et al., 1991; Etchberger and Hobert, 2008). The 3 kb *clhm-1* promoter::*clhm-1*::*gfp*::*unc-54* 3′UTR construct pJT44 was injected and chromosomally integrated using Mos1 single-copy insertion (Frøkjaer-Jensen et al., 2008) to create the transgene *drSi33* to examine CLHM-1 localization. To further study CLHM-1 localization in the body-wall muscles, the *myo-3* promoter::*clhm-1*::*gfp*::*unc-54* 3′UTR construct pJT19 was injected at 20 ng/μl with *myo-3* promoter::DsRed2 (pJer1; 50 ng/μl) and the coinjection marker pRol-6 (100 ng/μl).

Body-wall muscle cell-specific expression construct pJT48, created by inserting the *clhm-1* genomic sequence directly in frame with the *myo-3* promoter, was chromosomally integrated with the Mos1 insertion technique (Frøkjaer-Jensen et al., 2008) to generate the single copy insertion (SCI) transgene *drSi34* used for rescue experiments (see Fig. 5). The body-wall muscle cell-specific expression construct pJT41 was created by inserting the human *Calhm1* cDNA directly in frame with the *myo-3* promoter. This construct was chromosomally integrated with the Mos1 insertion technique (Frøkjaer-Jensen et al., 2012) to generate transgene *drSi51* used for rescue experiments (see Fig. 5).

For body-wall muscle overexpression experiments, the *myo-3* promoter::*clhm-1*::*unc-54* 3′UTR was amplified off of pJT48 and injected at 2 or 20 ng/μl, with pJer1 at 50 ng/μl as a coinjection marker. The *clhm-1* promoter::*clhm-1*::*clhm-1* 3′ UTR sequence was amplified off of genomic DNA and injected at 100 ng/μl with pJer1 at 50 ng/μl. Control lines were isolated by injecting pJer1 alone at 50 ng/μl. A multicopy array created by injection of pJT48 at 20 ng/μl with pJer1 at 50 ng/μl was isolated and then integrated by growing injected animals and subsequent generations on *clhm-1* RNAi (Source Biosource) to create *drIs22*.

To overexpress *clhm-1* in the touch neurons, an *mec-4* promoter::*clhm-1*::*unc-54* 3′UTR PCR product was amplified from pJT47 and injected at 2 ng/μl (unless noted otherwise) with an *mec-4* promoter::*mCherry*::*unc-54* 3′UTR PCR product (10 ng/μl) and the pRol-6 coinjection marker (100 ng/μl). Wild-type, *cnx-1(ok2234)*, and *crt-1(ok948)* animals that had been crossed with *zdIs5* (an integrated touch neuron marker, *mec-4p::GFP*) were injected on the same day, with the same injection mix and needle. The *mec-4* promoter::*hCalhm1 cDNA*::*unc-54* 3′UTR PCR product was amplified from pJT51, the *mec-4* promoter::*hCalhm1 P86L cDNA*::*unc-54* 3′UTR PCR product was amplified from pJT52, and the *mec-4* promoter::*mec-4(d)* PCR product was amplified from a construct supplied by M. Driscoll (Rutgers University, Piscatawa, NJ). These PCR products were injected at 2 ng/μl with *mec-4* promoter::*mCherry*::*unc-54* 3′UTR and pRol-6 as detailed above for *clhm-1*. Control animals were injected with the *mec-4* promoter::*mCherry*::*unc-54* 3′UTR PCR product (12 ng/μl) and pRol6 (100 ng/μl). At least five independent lines were analyzed for each genotype; animals containing mosaic neurons (GFP+, mCherry−) were excluded from the analysis.

Immunocytochemical staining. Adult wild-type and *myo-3* promoter::*hCalhm1* cDNA::*unc-54* 3′ UTR SCI *C. elegans* were prepared for staining using the previously described freeze-crack protocol, followed by a methanol/acetone fixation (Duerr et al., 1999; Gendrel et al., 2009). Staining was performed following the method used by Gendrel et al. (2009), with anti-CALHM1 antibodies (Sdix) at a 1:400 dilution and an Alexa-594-labeled donkey anti-rabbit IgG secondary antibody (Invitrogen) at 1:1000.

Fluorescence microscopy. C. elegans were immobilized with 10 mM levamisole (Sigma) on 3% agar pads. *clhm-1* expression pattern images

were obtained with a Zeiss LSM 510 confocal microscope. Animals with the *clhm-1* promoter::*gfp* transgene were exposed to the lipophilic fluorescent dye DiI and analyzed with a Leica DMI4000B inverted microscope to identify sensory neurons that expressed *clhm-1* (Tong and Bürglin, 2010). Images of touch neurons, CLHM-1::GFP localization, and human CALHM1 localization were obtained using a Leica DMI4000B inverted microscope (63× objective) with a Leica DFC340FX digital camera. The area and average intensity of CLHM-1::GFP fluorescence were determined using ImageJ software. Statistical significance was determined using one-way ANOVA with Dunnett's multiple comparison test.

Mechanics. A MATLAB-based image analysis and biomechanics algorithm was used to quantify *C. elegans* motility (Sznitman et al., 2010; Krajacic et al., 2012). Groups of one to three young adult worms grown at 25°C were transferred into a 50 μl drop of M9 buffer in the recording chamber and, after 2 min of acclimation, covered with a cover glass (catalog #12-544-10; Fisher Scientific). Recordings of *C. elegans* swimming for 4–10 s in the chamber were obtained with a Leica MZ16FA microscope equipped with a Leica DFC 340 FX camera using standard bright-field microscopy at 15 frames per second. For each recording, worm curvature (envelope of motion) was captured and plotted over time. Worm speed, force, and power calculations were performed in MATLAB (Sznitman et al., 2010; Krajacic et al., 2012). All analyses were performed blind to genotype. Statistical significance was determined using one-way ANOVA with Dunnett's multiple comparison test.

Touch neuron analysis. The numbers of visible PLM and ALM touch neurons were counted as GFP-positive cells every 3 h using a Leica DMI4000B inverted microscope (63× objective) during the L1 stage starting 14 h after the end of a 1 h pulse lay. Images of PLM touch neurons (see Fig. 6*A–C*) were taken 18–20 h after pulse lay. For animals at the fourth larval stage (L4), the presence/absence of each neuron was recorded. To determine whether EGTA or *crt-1* or *cnx-1* mutations could suppress the *clhm-1* overexpression phenotype, animals which hatched from eggs laid in a 1 h pulse lay period were analyzed either 22 h later or as L4 larvae. Animals that did not contain the transgene in all touch neurons (i.e., those with GFP-positive touch neurons not expressing the mCherry marker) were not analyzed. Touch sensitivity was determined by response to an initial anterior touch. Statistical significance was determined using Student's *t* test.

Muscle toxicity analysis. The viability of the *myo-3* promoter::*clhm-1*, *clhm-1* promoter::*clhm-1*, and *myo-3* promoter::*DsRed2* lines was determined by screening stable lines expressing DsRed2 in the F2 generation; a line was classified as nonviable if none of the animals expressing DsRed2 reached adulthood. A *myo-3* promoter::*clhm-1*::*unc-54* 3′UTR extrachromosomal array line was integrated into the genome using UV bombardment and subsequently outcrossed four times to generate strain OG471 *drIs22* [*myo-3 promoter::clhm-1::unc-54 3′ UTR; myo-3 promoter::DsRed2::unc-54 3′ UTR*]. This strain is only viable when grown on *clhm-1* RNAi. To identify extragenic suppressors of toxicity, five animals grown on *clhm-1* RNAi plates were transferred to empty vector, *clhm-1*, *cnx-1*, or *crt-1* RNAi (Source Biosource) as L4 animals, and the time of flight (i.e., size) of the offspring of these animals was measured with a COPAS Biosort (Union Biometrica) 72 h later (Morton and Lamitina, 2010).

Results

C. elegans CLHM-1 exhibits functional ion channel properties similar to human CALHM1

Heterologously expressed human CALHM1 displays properties consistent with it being the pore-forming subunit of a novel ion channel (Ma et al., 2012). Since *C. elegans* CLHM-1 is only 16% identical/28% similar at the amino acid level to human CALHM1, it was unclear whether the two proteins would exhibit similar functional properties. To determine whether *C. elegans* CLHM-1 is an ion channel in the plasma membrane, we first analyzed CLHM-1::GFP expressed in *Xenopus* oocytes and observed localization of CLHM-1 at or near the plasma membrane (Fig. 1*A*). We then recorded whole-cell currents from *Xenopus* oocytes injected with *C. elegans clhm-1* cRNA using protocols established previously by Ma et al. (2012). Membrane depolarization of CLHM-1-expressing oocytes in 2 mM Ca^{2+} solution produced large outward currents that deactivated upon stepping to hyperpolarized voltages (Fig. 1*B*). These currents were CLHM-1-dependent, since similar currents were not observed in control oocytes recorded under the same conditions (Fig. 1*C*). Thus, plasma membrane expression of *C. elegans* CLHM-1 in *Xenopus* oocytes produces voltage-dependent, outwardly rectifying currents.

To establish which ions are responsible for the currents observed in CLHM-1-expressing oocytes, we estimated relative permeabilities from reversal potential (E_{rev}) measurements (for pulse protocol, see Fig. 3*D*). Changing bath NaCl concentration in nominally Ca^{2+}-free solution caused a shift in E_{rev} values that were used in the Goldman–Hodgkin–Katz equation to calculate relative permeabilities P_{Na}:P_K:P_{Cl} = 1:1.09:0.51 (Fig. 1*D*). Relative Na^+, K^+, and Cl^- permeabilities were unchanged in the presence of 2 mM Ca_o^{2+}, suggesting that Ca_o^{2+} does not alter CLHM-1 ion selectivity (Fig. 1*D*). Increasing Ca_o^{2+} or Mg_o^{2+} in solutions containing constant NaCl shifted E_{rev} to more depolarized voltages, with relative permeabilities P_{Na}:P_{Ca}:P_{Mg} = 1:3.63:1.74 (Fig. 1*E*,*F*). Thus, like human CALHM1 (Ma et al., 2012), *C. elegans* CLHM-1 is permeable to monovalent cations, divalent cations, and anions with selectivity $Ca^{2+} > Mg^{2+} > Na^+ = K^+ > Cl^-$.

C. elegans clhm-1 encodes an ion channel

Although currents were observed only in CLHM-1-expressing oocytes and not in control oocytes, CLHM-1 could either be an ion channel or activate endogenous *Xenopus* ion channels. To distinguish between these possibilities, we mutated potential pore-lining residues and determined relative Ca^{2+} permeability. A change in ion selectivity for any of the mutant CLHM-1 proteins would be consistent with CLHM-1 being a pore-forming ion channel subunit. Acidic residues have been shown to influence ion selectivity of Ca^{2+}-permeable ion channels (Catterall 1993; Keramidas et al., 2004). Charge neutralization of the conserved residue Asp125 to Ala (D125A) caused a change in relative Ca^{2+} and Cl^- permeabilities from P_{Ca}:P_{Na}:P_K:P_{Cl} = 3.63:1:1.09:0.51 for wild-type CLHM-1 to P_{Ca}:P_{Na}:P_K:P_{Cl} = 1.83:1:1.02:0.90 for CLHM-1(D125A) (Fig. 1*F–H*). Mutation of the homologous Asp in human CALHM1 also altered ion selectivity (Ma et al., 2012), indicating that this residue plays an evolutionarily conserved role in Ca^{2+} permeability. As a second approach to show that CLHM-1 is an ion channel, we expressed *C. elegans* CLHM-1 in a different heterologous expression system, the *Axolotyl* oocyte. CLHM-1-expressing *Axolotyl* oocytes generated outwardly rectifying, voltage-dependent currents similar to those observed in CLHM-1-expressing *Xenopus* oocytes (data not shown). This further argues against the possibility that expression of CLHM-1 simply activates endogenous *Xenopus* conductances. Together, our results are consistent with CLHM-1 being a bona fide ion channel and suggest that a conserved Asp residue at the extracellular end of TM3 may line the channel pore.

CLHM-1 exhibits unique pharmacological properties

Since *C. elegans* CLHM-1 exhibits properties consistent with it being an ion channel, we sought to determine whether known channel inhibitors altered CLHM-1 currents. The relatively nonspecific blockers Gd^{3+} and Ruthenium red irreversibly inhibited CLHM-1 currents, while Zn^{2+} caused partially reversible inhibition (Fig. 2*A*,*B*,). The NMDA receptor blocker MK801 (Karp et al., 1993), L-type VGCC blocker nimodipine (Xu and Lipscombe, 2001), $InsP_3$ receptor and SOCE inhibitor 2-APB (Maruyama et

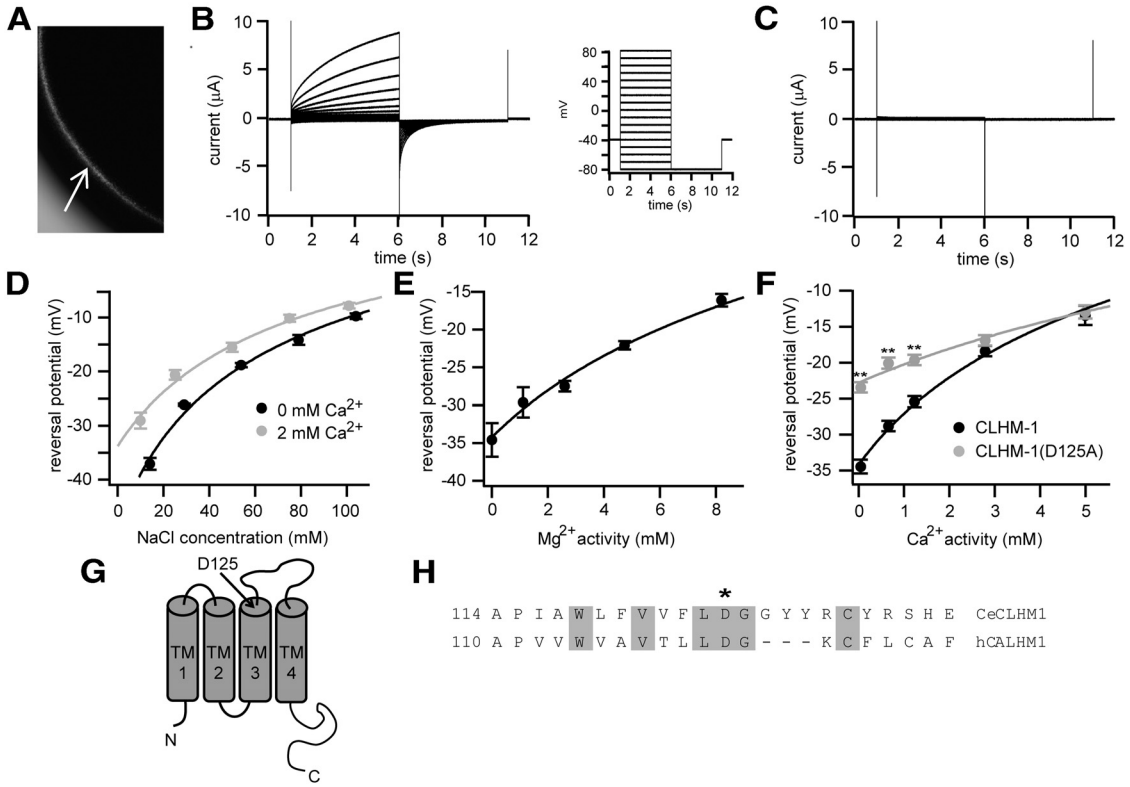

Figure 1. *C. elegans* CLHM-1 is a Ca^{2+} permeable ion channel. ***A***, CLHM-1::GFP localized to the plasma membrane (arrow) of *Xenopus* oocytes. ***B***, Currents observed in oocytes expressing *C. elegans* CLHM-1 in standard bath solution containing 2 mM Ca^{2+} in response to voltage pulses from −80 to +80 mV with a holding potential of −40 mV. ***C***, Using the same pulse protocol as in ***B***, currents were not observed in H_2O-injected control oocytes. All oocytes were injected with an antisense *Xenopus* Cx38 oligonucleotide and BAPTA to inhibit endogenous currents (Ma et al., 2012). ***D–F***, Reversal potentials (E_{rev}) determined by activating CLHM-1 at +60 mV and then measuring the instantaneous *I–V* relationship after stepping to different voltages over a range of NaCl concentrations in the absence (black) and presence (gray) of Ca_o^{2+} (***D***), Mg^{2+} activities (***E***), and Ca^{2+} activities (***F***). Solid lines show fit as determined by the extended GHK equation, used to calculate all relative permeability ratios. ***D***, $P_{Na}:P_K:P_{Cl} = 1:1.09 \pm 0.02:0.49 \pm 0.05$ in the absence of Ca_o^{2+}, and $P_{Na}:P_K:P_{Cl} = 1:1.06 \pm 0.02:0.55 \pm 0.05$ in the presence of 2 mM Ca_o^{2+}. ***E***, $P_{Na}:P_K:P_{Cl}:P_{Mg} = 1:1.15 \pm 0.01:0.49 \pm 0.02:1.74 \pm 0.09$. ***F***, $P_{Na}:P_K:P_{Cl}:P_{Ca} = 1:1.09 \pm 0.02:0.51 \pm 0.03:3.63 \pm 0.21$ for wild-type CLHM-1 (black), and $P_{Na}:P_K:P_{Cl}:P_{Ca} = 1:1.02 \pm 0.06:0.90 \pm 0.03:1.83 \pm 0.13$ for CLHM-1(D125A) (gray). $n \geq 5$ oocytes for each condition. Error bars indicate SE. $^{**}p < 0.01$. ***G***, Predicted topology of *C. elegans* CLHM-1, with Asp125 located on the extracellular side of TM3. ***H***, Alignment of the TM3 region. The star indicates the position of the conserved Asp residue.

al., 1997; Bootman et al., 2002), TRP channel blocker SKF96365 (Boulay et al., 1997), Cl^- channel blocker niflumic acid (White and Aylwin, 1990), and SERCA blocker thapsigargin (Lytton et al., 1991) did not affect CLHM-1 currents (Fig. 2*B*). These pharmacological properties are similar to those observed for human CALHM1 (Dreses-Werringloer et al., 2008; Ma et al., 2012). Strikingly, the connexin and pannexin hemichannel blockers octanol and carbenoxolone (Saez et al., 2003) caused a twofold increase in CLHM-1 currents (Fig. 2*A*,*B*). These pharmacological properties are distinct from other known channels, supporting the hypothesis that *C. elegans* CLHM-1 belongs to a unique family of ion channels.

CLHM-1 is regulated by extracellular Ca^{2+} and membrane voltage

Removal and subsequent add-back of Ca_o^{2+} has been shown to cause a dramatic increase in intracellular Ca^{2+} (Ca_i^{2+}) levels in cell lines expressing human CALHM1 (Dreses-Werringloer et al., 2008; Ma et al., 2012). This likely occurs because lowering Ca_o^{2+} activates human CALHM1 channels at resting membrane potentials (Ma et al., 2012). To determine whether Ca_o^{2+} alters the gating of *C. elegans* CLHM-1, we recorded currents from CLHM-1 expressing oocytes in divalent-free (Fig. 3*A*), 5 mM Ca^{2+} (*B*), and 5 mM Mg^{2+} (*C*) bath solutions. Compared with CLHM-1 currents observed in the presence of either Ca_o^{2+} or Mg_o^{2+}, CLHM-1 currents activated much more rapidly in the absence of divalent cations (Fig. 3*A–C*). This regulation by Ca_o^{2+} and Mg_o^{2+} was completely reversible (Fig. 2*A*; data not shown). These results indicate that CLHM-1 gating is regulated by both voltage and extracellular divalent cations.

While our results suggest that Ca_o^{2+} regulates CLHM-1 gating, the mechanism by which Ca_o^{2+} has this effect is unclear. Fast channel pore block that physically impedes ion flow leads to nonlinear instantaneous *I–V* relationships. To determine whether Ca_o^{2+} acts as a voltage-dependent fast pore blocker of CLHM-1, similar to the voltage-dependent pore block of NMDA receptors by Mg_o^{2+} (Mayer et al., 1984; Nowak et al., 1984), we measured currents in the presence and absence of Ca_o^{2+} using an instantaneous *I–V* pulse protocol. The instantaneous *I–V* relationships were linear in both the presence and absence of Ca_o^{2+} (Fig. 3*D*). Therefore, Ca_o^{2+} does not regulate CLHM-1 gating through a voltage-dependent fast pore-block mechanism.

To further analyze the effects of Ca_o^{2+} and voltage on gating regulation, we determined the apparent conductance–voltage (*G–V*) relationships for CLHM-1 in both divalent-free and various Ca_o^{2+} containing solutions. Using Boltzmann equations to fit the apparent *G–V* relationships, we determined that 5 mM Ca_o^{2+} right-shifted the apparent *G–V* relationship by ~75 mV from a half-activation voltage ($V_{0.5}$) of −6.8 mV in 0 mM Ca_o^{2+} to +69.1 mV in 5 mM Ca_o^{2+} (Fig. 3*E*). Similarly, 5 mM Mg_o^{2+} right-shifted

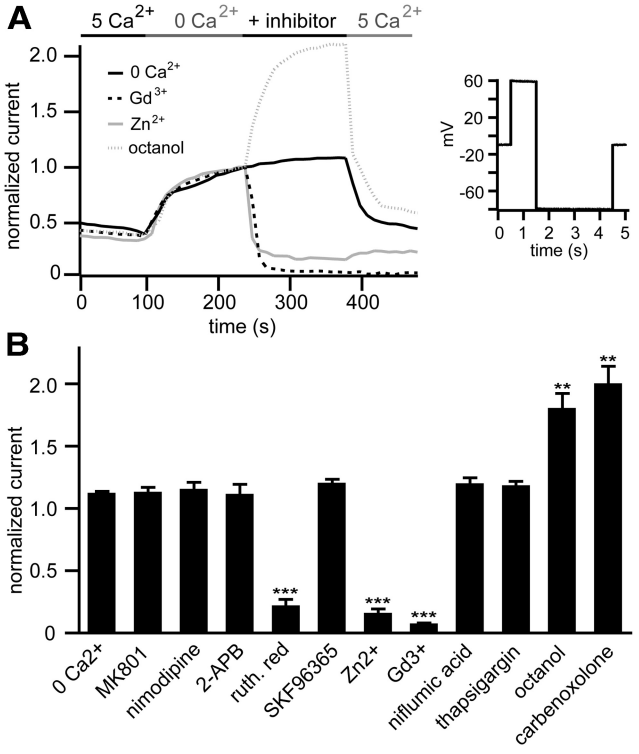

Figure 2. CLHM-1 exhibits unique pharmacological properties. ***A***, Shown are representative traces of CLHM-1 current inhibition by 100 μM Gd^{3+} (black dotted line) and 100 μM Zn^{2+} (gray solid line) and activation by 1 mM octanol (gray dotted line) compared with current in an oocyte maintained in 0 mM Ca^{2+} bath solution (black solid line). CLHM-1 currents were activated by depolarization to +60 mV, with tail currents measured at −80 mV. This was repeated ≥50 times at 10 s intervals for each oocyte, with solution changes as indicated. ***B***, Summary of pharmacological responses, with currents measured at 350 s normalized to currents immediately before inhibitor application; $n = 4–6$ oocytes (mean ± SE). MK801 (100 μM), $n = 4$; nimodipine (10 μM), $n = 4$; 2-APB (1 mM[SCAP]), $n = 5$; Ruthenium red (80 μM), $n = 4$; SKF96365 (50 μM), $n = 4$; Zn^{2+} (100 μM), $n = 4$; Gd^{3+} (100 μM), $n = 5$; niflumic acid (200 μM), $n = 4$; thapsigargin (100 nM), $n = 4$; octanol (1 mM), $n = 6$; and carbenoxolone (200 μM), $n = 6$. $^{**}p < 0.01$; $^{***}p < 0.001$.

the apparent *G–V* relationship by 62 mV (data not shown). The IC_{50} for Ca_o^{2+} was 184.3 ± 51.2 μM, with a Hill coefficient of 0.88 ± 0.2. Ca_o^{2+} did not appear to significantly affect the voltage-dependent slope (Fig. 3*E*), suggesting that Ca_o^{2+} may not directly affect the voltage-dependent gating. However, since the current was still in a rising phase at the end of the depolarizing pulses, our analysis of the apparent *G–V* relationship (Fig. 3*E*) does not exclude the possibility that Ca_o^{2+} could in fact affect voltage-dependent gating. Although using longer depolarizing pulses to address this problem was not possible due to instability of the oocytes and endogenous currents activated by such pulses, we note that our data are directly comparable to the apparent *G–V* relationship for human CALHM1, which was determined using the same protocol (Ma et al., 2012). In conclusion, our results indicate that Ca_o^{2+} regulates CLHM-1 gating by stabilizing CLHM-1 channels in the closed state at hyperpolarized voltages.

C. elegans CLHM-1 is expressed at the cell surface of excitable cells

RT-PCR has suggested that human *Calhm1* is primarily expressed in the brain and spinal cord, and *in situ* hybridization showed *Calhm1* expression in TRPM5-expressing taste cells (Dreses-Werringloer et al., 2008; Moyer et al., 2009; Taruno et al., 2013). Overexpression of human *Calhm1* in CHO cells resulted in plasma membrane and endoplasmic reticulum localization (Dreses-Werringloer et al., 2008); however, an analysis of the expression pattern and subcellular localization of mammalian CALHM proteins has not been performed *in vivo*. To determine the expression pattern of *clhm-1* in *C. elegans*, we generated transgenic worms expressing a transcriptional reporter consisting of a 3kb *clhm-1* promoter region followed by *gfp*. We observed GFP expression in head and body-wall muscles; IL2, ASG, ASI, ASJ, PHA and PHB sensory neurons; and the spermatheca (Fig. 4*A–C*).

To examine the localization of the CLHM-1 protein, we inserted a single copy *clhm-1* promoter::*clhm-1*::*gfp* translational fusion construct into the *C. elegans* genome. When expressed in *Xenopus* oocytes, CLHM-1::GFP produced an ion conductance indistinguishable from untagged CLHM-1, suggesting that the presence of a C-terminal GFP tag does not interfere with CLHM-1 channel localization or function (data not shown). CLHM-1::GFP at single copy localized to ciliary endings of sensory neurons and in a punctate pattern at or near the plasma membrane of muscles (Fig. 4*D*; data not shown). To further investigate the localization of CLHM-1 in muscles, we expressed DsRed2 in the cytoplasm of the body-wall muscles along with a multicopy *myo-3* promoter::*clhm-1::gfp* translational fusion construct. The CLHM-1::GFP and DsRed2 fluorescence were not colocalized, further demonstrating CLHM-1 localization at or near the plasma membrane (Fig. 4*E–G*).

Although the ion channel function of the CLHM-1::GFP fusion protein is indistinguishable from untagged CLHM-1, it is possible that the GFP tag alters the subcellular distribution of CLHM-1 in a way that forces its accumulation at or near the plasma membrane. A CLHM-1-specific antibody to localize endogenous CLHM-1 could distinguish between these possibilities, although our initial attempts at developing such a reagent were unsuccessful (data not shown). As an alternative approach, we expressed a functional human *Calhm1* transgene (Fig. 5*D–F*) at single copy in the body-wall muscles and performed immunofluorescence to determine the CALHM1 localization pattern using a commercially available antibody. Consistent with the localization pattern observed with CLHM-1::GFP, CALHM1 localized to the plasma membrane at body-wall muscle intercellular junctions as well as in the muscle arms and synaptic regions (Fig. 4*H–I*). These data suggest that CALHM family members are primarily localized at or near the plasma membrane of excitable cells and represent the first *in vivo* description of the physiological expression pattern and localization of a CALHM family member.

CLHM-1 mutants exhibit uncoordinated locomotion

While genetic studies suggest that a polymorphism in human *Calhm1* results in pathophysiological consequences (Dreses-Werringloer et al., 2008; Boada et al., 2010; Lambert et al., 2010), phenotypes associated with loss of *Calhm1* expression have not been determined. To examine the physiological role(s) of CLHM-1 in *C. elegans*, we obtained two knock-out mutants, *clhm-1(ok3617)* and *clhm-1(tm4071)*. Both deletions remove a significant section of the transmembrane domain region, resulting in predicted null alleles (Fig. 5*A*). Since a primary site of *clhm-1* expression is the body-wall muscles and these cells control motility, we quantified the swimming gait of outcrossed *clhm-1* mutants using a quantitative fluid mechanics approach (Sznitman et al., 2010; Krajacic et al., 2012). Loss of *clhm-1* significantly disrupted some, but not all, kinematic parameters, including mean wave speed (Fig. 5*B,C*), suggesting that loss of *clhm-1* af-

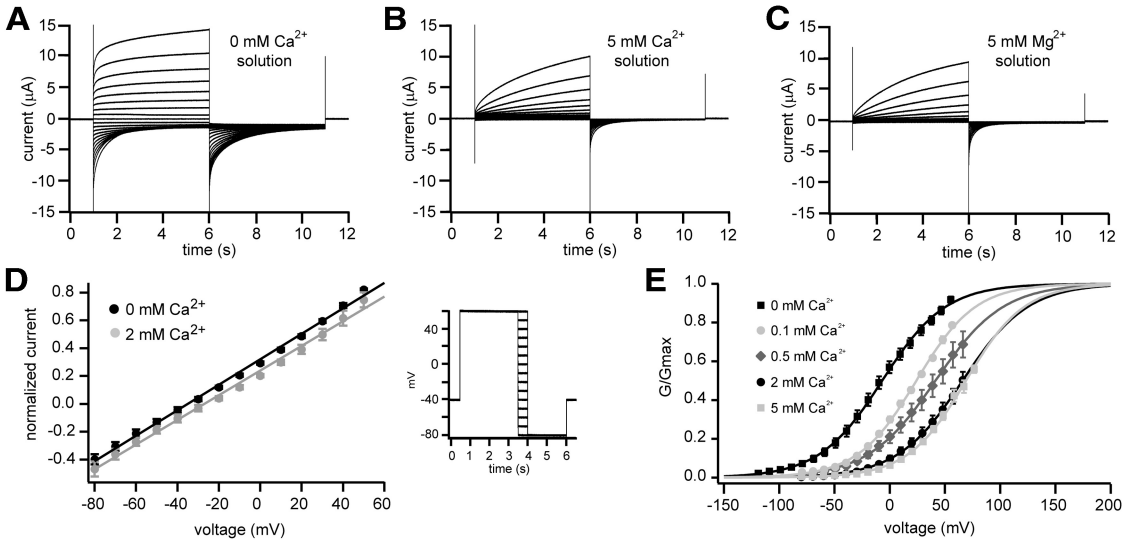

Figure 3. *C. elegans* CLHM-1 is regulated by voltage and extracellular divalent cations. ***A***, Currents observed in oocytes expressing *C. elegans* CLHM-1 in response to voltage pulses from −120 to +60 mV. The holding potential was at the resting potential (ranged from −5 to −15 mV) in divalent-free bath solution containing 0.5 mM EGTA and 0.5 mM EDTA. ***B***, ***C***, Using the same protocol as in Figure 1*B*, currents observed in oocytes expressing *C. elegans* CLHM-1 in standard bath solution containing 5 mM Ca^{2+} (***B***) or 5 mM Mg^{2+} (***C***). All oocytes were injected with the Cx38 oligonucleotide and BAPTA to inhibit endogenous currents (Ma et al., 2012); currents were not observed in H_2O-injected oocytes in the presence or absence of divalent cations (Fig. 1*C*; data not shown). ***D***, Instantaneous current–voltage relationship in divalent-free (black) and 2 mM Ca^{2+} (gray) bath solutions. Tail currents observed after stepping to the different voltages were normalized to average current at the end of the activating +60 mV prepulse; solid lines show linear fit. ***E***, CLHM-1 currents at −80 mV were measured after a series of voltage steps (as in ***A***, ***B***) to determine conductance–voltage relationships in the absence and presence of Ca_o^{2+}. The currents in various Ca_o^{2+} solutions were normalized to G_{max} determined by fitting 0 mM Ca_o^{2+} data with a Boltzmann function for each oocyte. All normalized data were then fit with Boltzmann functions (lines) as for human CALHM1 (Ma et al., 2012) with the assumption that Ca_o^{2+} does not affect G_{max}. This fit gave rise to the apparent conductance–voltage relationship. Half-activation voltages are as follows: 0 mM Ca_o^{2+} (black squares), $V_{0.5} = -6.8 \pm 0.4$ mV; 0.1 mM Ca_o^{2+} (light gray circles), $V_{0.5} = 24.1 \pm 0.4$ mV; 0.5 mM Ca_o^{2+} (dark gray diamonds), $V_{0.5} = 41.4 \pm 0.3$ mV; 2 mM Ca_o^{2+} (black circles), $V_{0.5} = 66 \pm 0.4$ mV; 5 mM Ca_o^{2+} (light gray squares), $V_{0.5} = 69.1 \pm 0.5$ mV. $n \geq 5$ oocytes for each condition. Error bars show the SE of normalized data.

fects specific aspects of the swim gait. The kinematic defects observed in both *clhm-1* mutants caused reduced forward velocity and diminished muscle force and power production compared to wild-type worms (Fig. 5*D–F*).

To test whether the biomechanical defects were caused by loss of *clhm-1* expression in muscle, we transgenically expressed *C. elegans* CLHM-1 in the body-wall muscles of the *clhm-1* mutant and determined whether this could rescue the locomotion defects. Expression of a body-wall muscle promoter::*clhm-1* single-copy transgene did not cause a significant biomechanical phenotype in the wild-type background (Fig. 5*C–F*), while expression in the *clhm-1* mutant worms was sufficient to rescue the defects in forward velocity, force, and power production (Fig. 5*D–F*). Despite exhibiting only 16% sequence identity with *C. elegans* CLHM-1, single-copy muscle-specific expression of human CALHM1 was also sufficient to rescue the biomechanical defects of the *clhm-1* mutant, demonstrating that worm CLHM-1 and human CALHM1 are functionally conserved (Fig. 5*D–F*). In summary, our results demonstrate that CLHM-1 acts in the body-wall muscles to maintain normal motility and show that the function of *Calhm* family members is evolutionarily conserved.

Overexpression of CLHM-1 in the *C. elegans* touch neurons induces neurodegeneration

Mutation of human *Calhm1* has been associated with LOAD (Dreses-Werringloer et al., 2008; Boada et al., 2010; Lambert et al., 2010), which is characterized by neuronal dysfunction and degeneration, yet the consequences of overexpression of mammalian CALHM proteins *in vivo* have not been determined. We explored the effects of *clhm-1* overexpression in neurons even though we have not yet identified a phenotype associated with loss of neuronal *clhm-1* (data not shown). Although not a site of endogenous *clhm-1* expression, the *C. elegans* touch neurons are a well-established model for studying the impact of toxic ion channels on neuron function and death (Driscoll and Chalfie, 1991; Chung et al., 2000; Xu et al., 2001; Syntichaki et al., 2002). Overexpression of *clhm-1* in the touch neurons caused swelling and degeneration of the ALM and PLM neurons during the first larval (L1) stage (Fig. 6*A–D*), similar to the effect of dominant mutations in the DEG/ENaC channel *mec-4(d)* (Driscoll and Chalfie, 1991; Xu et al., 2001). This rapid neurodegeneration was not simply a general response to increased ion channel expression, since overexpression of wild-type *mec-4* or another DEG/ENaC channel, *mec-10(d)*, is not sufficient to cause touch insensitivity or touch neuron degeneration, respectively (Royal et al., 2005; Zhang et al., 2008). Thus, overexpression of *clhm-1* specifically induces cell swelling and neurodegeneration characteristic of pathophysiologically induced necrotic cell death.

Overexpression of *C. elegans* CLHM-1, human CALHM1, or LOAD-associated P86L human CALHM1 caused completely penetrant degeneration of the AVM and pairs of PLM and ALM neurons by L4 (Fig. 6*E–H*). The PVM touch neurons, which are born at the end of the L1 stage and are not required for the touch response (Chalfie et al., 1985), were largely unaffected by overexpression of CALHM proteins (Fig. 6*E–H*). Higher expression of *clhm-1* was sufficient to induce PVM degeneration, suggesting that CLHM-1 toxicity is dose dependent (Fig. 6*H*; data not shown). To test whether the touch neurons in the CLHM-1-overexpressing animals were indeed absent, we performed touch assays on the transgenic worms. Consistent with loss of the touch neurons, animals that overexpressed *clhm-1* exhibited a touch-insensitive phenotype (Fig. 6*I*). Our results establish *Calhm* family members as conditionally toxic ion channels, capable of inducing necrotic-like neuronal death.

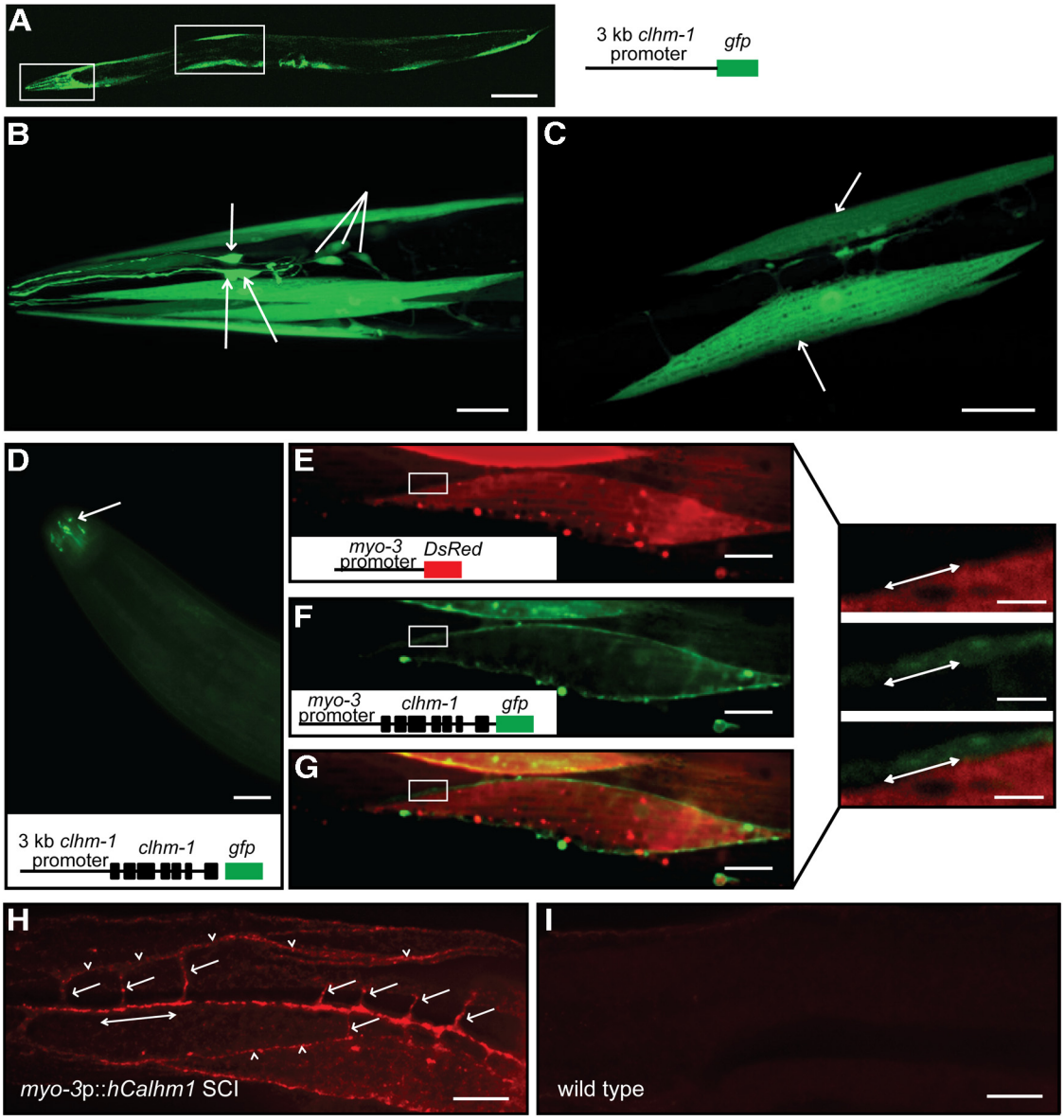

Figure 4. *C. elegans* CLHM-1 is expressed in excitable cells. ***A***, GFP fluorescence in animals carrying a *clhm-1* promoter::*gfp* transgene. ***B***, ***C***, This reporter transgene was expressed in many cells, including head muscles, IL2 neurons (arrows), and other sensory neurons (lines; ***B***), as well as the body-wall muscles (arrows; ***C***). ***D***, CLHM-1::GFP fluorescence localized to cilia of sensory neurons (arrow) in animals carrying a *clhm-1* promoter::*clhm-1*::*gfp* single-copy transgene. ***E***, ***F***, Overexpression of DsRed2 and CLHM-1::GFP, respectively, in the body-wall muscles. ***G***, Merge. Offset images on the right are magnifications of boxed areas in ***E–G***; the lines indicate the location where DsRed2 and CLHM-1::GFP fluorescence appear to meet, but not overlap. ***H***, Localization of human CALHM1 in animals carrying a rescuing *myo-3* promoter::*hCalhm1* transgene at single copy. Arrowheads point to muscle intercellular membranes, arrows point to muscle arms, and the double-headed arrow indicates the synaptic region. ***I***, CALHM1 staining is not present in wild-type animals. Scale bars: ***A***, 100 μM; ***B***, ***C***, 20 μm; ***D–I***, 10 μm; offset images, 3 μm.

Alteration of Ca^{2+} levels delays CLHM-1-induced neurodegeneration without affecting CLHM-1 expression

To determine the mechanism by which *clhm-1* overexpression leads to cell death, we looked for conditions that could suppress CLHM-1-induced neurodegeneration. Disruption of cellular Ca^{2+} balance by both chemical reagents and genetic mutations has been used to suppress the touch neuron necrosis observed in *mec-4(d)* mutants (Xu et al., 2001; Syntichaki et al., 2002). Growth of *clhm-1* overexpression animals in the presence of the Ca^{2+} chelator EGTA to reduce Ca_o^{2+} partially suppressed the *clhm-1* overexpression phenotype in the L1 stage, suggesting that Ca^{2+} plays a role in CLHM-1-induced cell death (Fig. 7*A*). To analyze the role of intracellular Ca^{2+} stores, we used a candidate gene approach and overexpressed *clhm-1* in calreticulin (*crt-1*) and calnexin (*cnx-1*) mutants. Loss of *crt-1* or *cnx-1* caused significant suppression of CLHM-1-induced neurodegeneration in L1 animals, but the remaining PLMs and ALMs still degenerated by the L4 stage (Fig. 7*A*,*B*). Thus, *crt-1* and *cnx-1* mutations were only sufficient to delay CLHM-1-induced neurodegeneration. In contrast, loss of *crt-1* or *cnx-1* was sufficient to suppress touch neuron degeneration induced by overexpression of *mec-4(d)* in L4 animals (Fig. 7*B*). These results indicate that Ca^{2+} signaling plays a role in CLHM-1-induced neurodegeneration; however, other mechanisms, including overall disruption of ion homeostasis or excitotoxicity, may also be contributing factors.

Since *crt-1* and *cnx-1* have dual functions in regulating ER Ca^{2+} homeostasis and protein folding (Coe and Michalak, 2009), it is

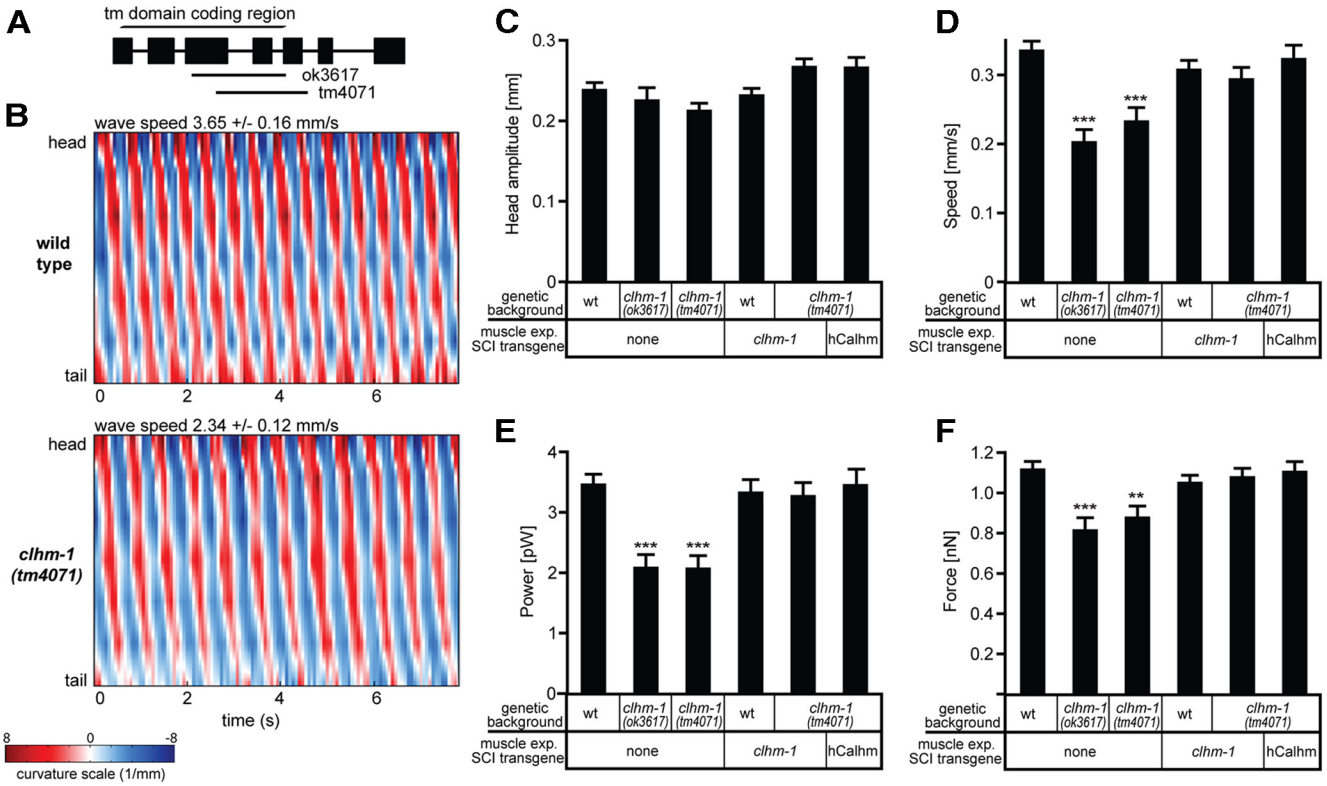

Figure 5. CLHM-1 is required for swimming locomotion. ***A***, Intron–exon structure for *C. elegans clhm-1*; locations of the *tm4071* and *ok3617* deletions as well as the transmembrane domain coding region are indicated. ***B***, Representative body curvature plots for wild-type and *clhm-1(tm4071)* mutant *C. elegans*. Average wave speed (speed at which the body bend propagates from head to tail) ± SD is significantly reduced in the *clhm-1* mutant. $p < 0.01$. ***C***, Average head amplitude exhibited no significant differences. $p > 0.05$. ***D–F*** Forward speed, mechanical power, and propulsive force are significantly decreased in *clhm-1* mutants. $^{**}p < 0.01$; $^{***}p < 0.001$ compared to wild-type worms. Expression of either *C. elegans clhm-1* or human *Calhm1* in the body-wall muscles of the *clhm-1(tm4071)* mutant using the single-copy transgene method rescued speed, power, and force defects. $p > 0.05$ compared to wild-type. For ***C–F***, $n \geq 10$ animals per genotype. Error bars indicate SD. All strains were recorded and analyzed blind to genotype at least two independent times; data presented are from a representative experiment.

possible that these mutations change surface expression levels of CLHM-1. To determine whether CLHM-1 expression levels were altered under any of the conditions tested, we measured CLHM-1::GFP fluorescence levels in animals grown in the presence of EGTA as well as in *crt-1* and *cnx-1* mutants. A significant decrease in the area as well as intensity of CLHM-1::GFP fluorescence was observed in the *cnx-1* mutant (Fig. 7*C*,*D*) indicating a decrease in CLHM-1 expression. The presence of EGTA and the *crt-1* mutation did not have a significant effect on CLHM-1::GFP fluorescence, suggesting that these manipulations likely delay CLHM-1-induced neurodegeneration by altering Ca^{2+} levels and not CLHM-1 expression (Fig. 7*C*,*D*). In conclusion, factors that regulate cellular Ca^{2+} levels and CLHM-1 surface expression can significantly delay the toxic effects of *clhm-1* overexpression.

Overexpression of CLHM-1 in a subset of endogenous cell types induces toxicity

While overexpression of CLHM-1 in the touch neurons demonstrates that this channel is capable of causing neurodegeneration, this result is based on expression of the channel in a nonnative cell type. We sought to determine whether CLHM-1 causes toxicity when overexpressed in a subset of cells where the endogenous channel is normally expressed. Overexpression of *clhm-1* in the body-wall muscles caused completely penetrant embryonic/L1 lethality that was suppressed by growing the animals on *clhm-1* RNAi, demonstrating that the toxicity was due to CLHM-1 (Fig. 8*A–D*). As observed with CLHM-1 overexpression in the touch neurons, the toxicity associated with overexpression in the body-wall muscles was dose dependent (Fig. 8*E*) and could be partially suppressed by loss of *cnx-1* (Fig. 8*F*). Overexpression of CLHM-1 from its endogenous promoter was also sufficient to cause lethality in a small percentage of transgenic lines (Fig. 8*E*). Interestingly, when we overexpressed CLHM-1 in the IL2 neurons, another subset of cells that express the endogenous channel, we did not observe neurodegeneration (data not shown). This suggests that some of the cells that normally express CLHM-1 may have mechanisms to deal with toxicity associated with high expression of the channel. Thus, overexpression of CLHM-1 in some, but not all of the cells where it is normally expressed, results in toxicity.

Discussion

In this work, we show that *C. elegans* CLHM-1 encodes an evolutionarily conserved ion channel, as human CALHM1 and *C. elegans* CLHM-1 exhibit similar biophysical properties when expressed in *Xenopus* oocytes and functional conservation when expressed in *C. elegans*. Based on our data demonstrating that CLHM-1 (1) is a bona fide ion channel, (2) exhibits a permeability preference for Ca^{2+}, (3) is regulated by membrane voltage and extracellular Ca^{2+}, and (4) is expressed at the surface of excitable cells, and that (5) CLHM-1 overexpression-induced neurodegeneration is delayed by lowering Ca^{2+} levels, we suggest that CALHM proteins are novel ion channels that sense and regulate Ca^{2+} signaling *in vivo*.

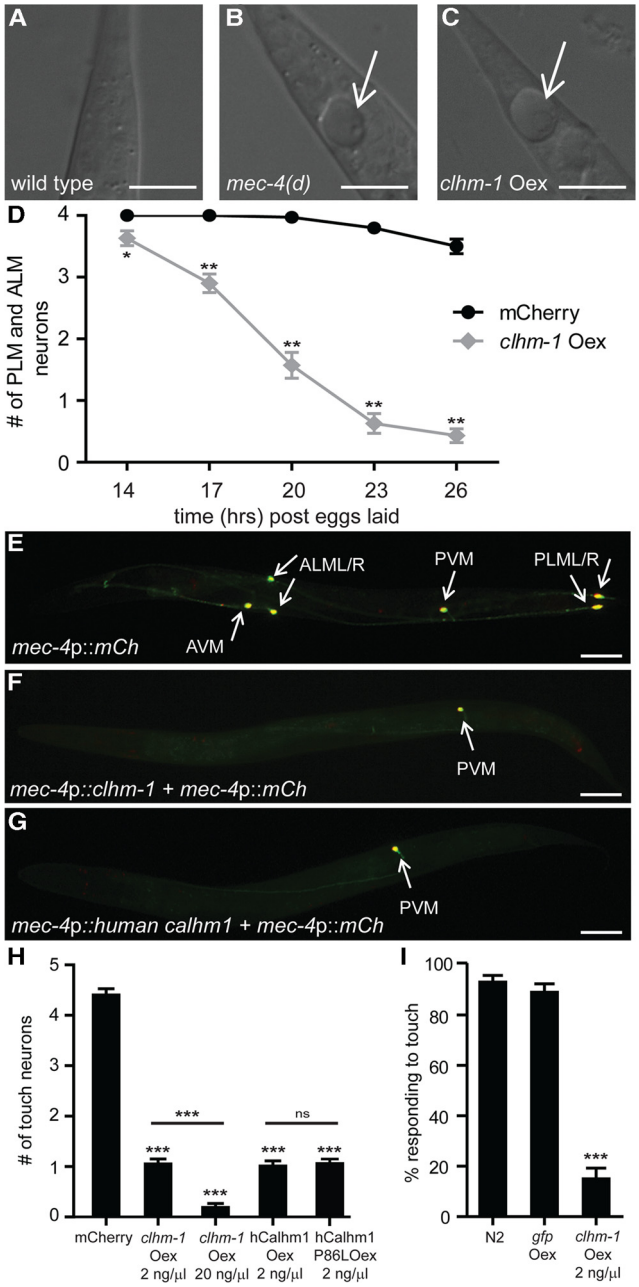

Figure 6. Overexpression of CALHM proteins is sufficient to cause neurodegeneration. ***A–C***, Nomarski images of the *C. elegans* tail show that both the *mec-4(d)* mutation (***B***) and overexpression of CLHM-1 (***C***) caused swelling of a PLM neuron (arrow). ***D***, Touch neuron overexpression of *clhm-1* (gray), but not mCherry (mCh; black), resulted in progressive and nearly complete loss of PLM and ALM neurons by the end of the L1 stage (26 h after eggs laid). $n = 30$ animals per genotype (6 animals from 5 independent transgenic lines). ***E***, L4 stage wild-type animals have six touch neurons (arrows): a pair of PLMs, a pair of ALMs, an AVM and a PVM. ***F***, ***G***, Overexpression of either *C. elegans clhm-1* or human *Calhm1* in the touch neurons caused degeneration of all touch neurons except the PVM (arrow). ***H***, Quantification of touch neuron degeneration; $n = 100$ animals per genotype (20 animals from five independent lines); ns, indicates not significant. ***I***, Overexpression of *clhm-1*, but not *gfp* caused loss of touch sensitivity as determined by response to an initial anterior touch; $n = 100$ animals per genotype. Scale bars: ***A–C***, 10 μm; ***E–G***, 50 μm. Error bars indicate SEM. ns, Not significant. $^*p < 0.05$; $^{**}p < 0.01$; $^{***}p < 0.001$.

CLHM-1 acts as an extracellular Ca^{2+} sensor

At times of high excitatory activity at synaptic clefts, local Ca_o^{2+} transiently becomes depleted due to NMDA receptor and VGCC activation (Rusakov and Fine, 2003). The sensitivity of CLHM-1 to voltage and Ca_o^{2+} suggests that it may act as a Ca_o^{2+} sensor to amplify neurotransmission. An emerging number of neuronal channels including hemichannels, the sodium leak channel NALCN, and other unidentified nonselective cation channels are capable of sensing physiological changes in Ca_o^{2+} (Xiong et al., 1997; Gómez-Hernández et al., 2003; Saez et al., 2003; Smith et al., 2004; Lu et al., 2010). Most recently, Ma et al. (2012) showed that human CALHM1 plays a role in the electrophysiological responses of cortical neurons to changes in Ca_o^{2+}. Compared with previously described channels that respond to Ca_o^{2+}, *C. elegans* CLHM-1 and human CALHM1 channels exhibit unique regulatory mechanisms, permeability properties, and sequences (Ma et al., 2012). In particular, the unusual regulatory properties and the neurodegeneration phenotype associated with overexpression of *Calhm* family members suggest that these channels may contribute to neuronal death associated with excitotoxic synaptic activity (MacDonald et al., 2006).

Although it is clear that Ca_o^{2+} plays a fundamental role in CLHM-1 regulation, we do not know how voltage or Ca_o^{2+} is sensed by the channel. Despite remarkable similarities in biophysical properties, there are some differences in the gating of *C. elegans* CLHM-1 compared to that of human CALHM1. Removal of Ca_o^{2+} shifted CALHM1 and CLHM-1 voltage-dependent activation toward hyperpolarized voltages; however, the magnitude of this shift was different for the two proteins (Ma et al., 2012). In addition, Ca_o^{2+} affected the voltage-dependence (G–V slope) of human CALHM1 (Ma et al., 2012), but not *C. elegans* CLHM-1. Given that neither human CALHM1 nor *C. elegans* CLHM-1 contain known Ca^{2+}-binding sequences or canonical voltage-sensing domains, defining the sequences underlying differences between the two proteins could reveal new molecular mechanisms for both voltage and Ca^{2+} sensing.

C. elegans CLHM-1 activity at the plasma membrane regulates excitable cell function

The power of the *C. elegans* model system has allowed us to address important unanswered questions concerning the subcellular localization and *in vivo* function of *Calhm* family members. For the first time, we defined the protein localization pattern of a CALHM family member *in vivo*. Comparison of the localization patterns of CLHM-1 and other proteins that regulate body-wall muscle function suggests that CLHM-1 does not localize to the same regions as the L-type VGCC EGL-19 (Kim et al. 2009), Shaker K^+ channel SHK-1 (Fawcett et al., 2006), or BK channel SLO-1 (Carre-Pierrat et al., 2006). While AChRs and GABA receptors are strictly localized to the synapse (Bamber et al., 1999; Gendrel et al., 2009), CALHM family members exhibit both synaptic and extrasynaptic localization like the innexin UNC-9 (Liu et al., 2006). CALHM proteins are similar in oligomeric structure, though not sequence, to connexins and innexins, but human CALHM1 cannot form gap junctions (Siebert et al., 2013). Since human CALHM1 can rescue the *C. elegans clhm-1* mutant biomechanical defects, our data suggest that the requirement for CLHM-1 in motility may depend more on its role as a plasma membrane ion channel than on another putative function(s).

Loss of *clhm-1* in the body-wall muscles caused an uncoordinated locomotion phenotype, demonstrating that this ion channel plays a physiologically significant role in regulating behavior. However, we still do not understand why loss of *clhm-1* results in locomotion defects. Biomechanical profiling (BMP) as conducted on *clhm-1* mutants was performed previously on 21 mutants with neuromuscular structure or signaling defects (Krajacic et al., 2012). Utilizing a clustering analysis, the biomechanical profile of a mutant can be used to predict gene function (Krajacic et al., 2012). Interestingly,

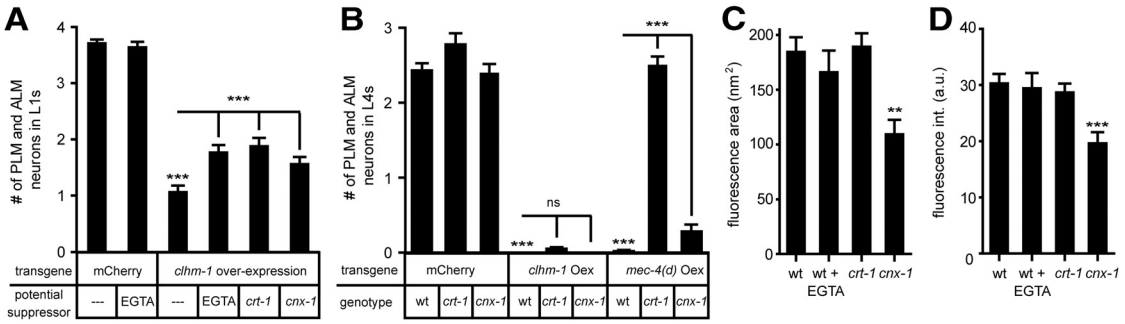

Figure 7. Reduction of extracellular Ca^{2+} and plasma membrane CLHM-1 expression delays CLHM-1-induced neurodegeneration. ***A***, Pharmacological and genetic manipulations were used to alter cellular Ca^{2+} levels. Growth of worms on 50 mM EGTA plates to reduce Ca_o^{2+} concentration partially suppressed CLHM-1-induced loss of PLM and ALM neurons in the L1 stage. Mutations in *crt-1* and *cnx-1*, which decrease release of Ca^{2+} from intracellular stores, also partially suppressed CLHM-1-induced neurodegeneration. ***B***, Analysis of animals in the L4 stage indicated that mutations in *crt-1* and *cnx-1* were not sufficient to suppress CLHM-1-induced cell death, while *mec-4(d)* overexpression was fully suppressed by loss of *crt-1* and partially suppressed by *cnx-1*. For ***A*** and ***B***, $n = 50$ animals (controls) or $n = 100$ animals from five independent lines (20 animals from each line). ***C***, ***D***, Quantification of CLHM-1::GFP fluorescence area (in square nanometers) and intensity in cilia of L4 animals expressing a *clhm-1* promoter::*clhm-1*::*gfp* single-copy transgene. $n \geq 30$ animals per genotype. Error bars indicate SEM. ns, Not significant. $^{**}p < 0.01$; $^{***}p < 0.001$.

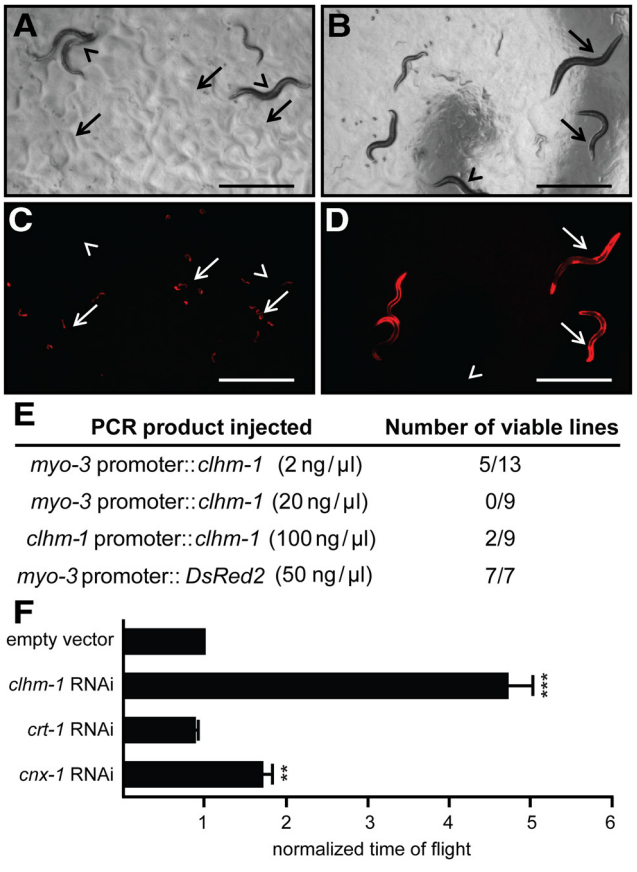

Figure 8. Overexpression of CLHM-1 in the body-wall muscles causes lethality. ***A–D***, Bright-field (***A***, ***B***) and fluorescent images (***C***, ***D***) of transgenic animals, identified by DsRed2 expression, with *clhm-1* overexpressed in the body-wall muscles. ***A***, ***C***, Animals grown on empty-vector RNAi. ***B***, ***D***, Animals grown on *clhm-1* RNAi. Arrowheads indicate nontransgenic animals that lack the DsRed2 marker; arrows indicate transgenic animals. Scale bars: 1000 μm. ***E***, Number of viable transgenic lines isolated when *clhm-1* was expressed from the body-wall muscle *myo-3* promoter and the endogenous *clhm-1* promoter. ***F***, Growth of *myo-3* promoter::*clhm-1*-overexpressing worms on the indicated RNAi bacterial clones. Normalized time of flight is a measure of worm length that corresponds to developmental stage. $n \geq 3$ independent experiments per RNAi clone; $n >$ 1000 animals per experiment. Data shown are mean ± SEM. $^{**}p < 0.01$; $^{***}p < 0.001$.

the *clhm-1* mutant biomechanical profile clustered with the synaptic signaling proteins and not the dystrophin-associated glycoprotein complex proteins (data not shown). Currently, only a limited number of mutants have been tested with BMP. Determining whether the biomechanical profile of *clhm-1* is similar to genes that regulate cell excitability, Ca^{2+} signaling, or electrical coupling between cells could help suggest a mechanism by which CLHM-1 regulates locomotion.

Coordinated muscle contraction and movement in *C. elegans* is regulated by a balance of synaptic acetylcholine and GABA signaling (Richmond and Jorgensen, 1999) as well as the electrical properties of the body-wall muscles (Liu et al., 2011a,b). Although *C. elegans* lack voltage-gated Na^+ channels (Bargmann, 1998), action potentials are generated in the body-wall muscles by Ca^{2+} entry through the L-type VGCC EGL-19 (Jospin et al., 2002; Liu et al., 2011a). Under physiological conditions, activity of many ion channels including the K^+ channels SHK-1 and SLO-2, the innexin UNC-9, the GABA receptor UNC-49, and subunits of the levamisole-sensitive AChR modulates action potentials in the muscles (Liu et al., 2011a,b). As loss of human CALHM1 in cortical neurons results in a decrease in the firing of action potentials (Ma et al., 2012), it is possible that loss of *C. elegans* CLHM-1 alters action potentials in the body-wall muscles, affecting locomotion.

While only a small number of channels function in the body-wall muscles under normal physiological circumstances, additional conductances are activated by more specific conditions (Santi et al., 2003). For example, SHL-1 and SHK-1 are responsible for most of the voltage-dependent K^+ conductance under physiological conditions (Fawcett et al., 2006), while an increase in intracellular Cl^- and Ca^{2+} activates the K^+ channel SLO-2 (Santi et al. 2003). We still do not know when CLHM-1 is active *in vivo*, and, in fact, it may only be activated under specific conditions, such as low Ca_o^{2+}. Future efforts will be directed toward determining whether loss of CLHM-1 under physiological or low Ca_o^{2+} conditions alters resting membrane potential, action potential firing, Ca^{2+} transients, and/or muscle morphology.

There are likely other phenotypes associated with *clhm-1* loss of function. Our work has shown that *C. elegans* CLHM-1 is expressed in several sensory neurons, analogous to human *Calhm1* expression in neurons and the sensory TRPM5-positive taste cells (Dreses-Werringloer et al., 2008; Moyer et al., 2009; Taruno et al., 2013).

While the Ca^{2+} permeability of human CALHM1 has been well established (Dreses-Werringloer et al., 2008; Ma et al., 2012), CALHM1 was shown previously to act as a voltage-gated ATP release channel required for sweet, bitter, and umami tastes (Taruno et al., 2013). Although *C. elegans* does not have P2X receptors that are activated by extracellular ATP (Khakh and North 2006), worms may have an alternative receptor that can be activated by ATP or CLHM-1 may release different substances. Understanding how CLHM-1 regulates the activity of the sensory neurons could provide insight into CLHM-1 function in a native neuronal context.

Calhm family members are Ca^{2+}-permeable, conditionally toxic ion channels

The P86L polymorphism in CALHM1 is likely a contributing, but not an independent, risk factor for LOAD (Lambert et al., 2010). While the P86L polymorphism has been shown to alter CALHM1-induced Ca^{2+} permeability and amyloid precursor protein processing in cell culture (Dreses-Werringloer et al., 2008), the mechanism by which aberrant CALHM1 signaling causes neuron dysfunction *in vivo* is unknown. Here we show that overexpression of *Calhm* family members in the *C. elegans* touch neurons is sufficient to induce necrotic-like neuronal death. *C. elegans* do not produce endogenous Aβ (Wu and Luo, 2005), suggesting that the mechanism by which neurodegeneration is induced is Aβ independent. Thus, it is possible that altered signaling through human CALHM1, which is regulated by and permeable to Ca^{2+}, could disrupt neuronal Ca^{2+} homeostasis and cause necrotic neuron death via an Aβ independent mechanism.

The proteins that regulate CALHM1 trafficking and function in humans, as well as those that act downstream of CALHM1, are completely unknown. While we have shown that manipulations which reduce release of Ca^{2+} from intracellular stores significantly delay the toxic effects of *clhm-1* overexpression, additional unidentified proteins and/or mechanisms likely also play a role since the neurons still die. Such mechanisms can be defined in *C. elegans* using unbiased forward genetic screens to identify mutants that suppress the toxicity associated with CLHM-1 overexpression. This genetic approach has the potential to identify novel and physiologically significant CALHM interactors in a way not currently possible in mammalian systems. Identification of CLHM-1 regulators in *C. elegans* will provide insights into the molecular mechanisms that control human CALHM1 localization and function as well as downstream proteins required for the conditionally toxic effects of CALHM signaling.

References

Bamber BA, Beg AA, Twyman RE, Jorgensen EM (1999) The *Caenorhabditis elegans unc-49* locus encodes multiple subunits of a heteromultimeric GABA receptor. J Neurosci 19:5348–5359. Medline

Bargmann CI (1998) Neurobiology of the *Caenorhabditis elegans* genome. Science 282:2028–2033. CrossRef Medline

Beecham GW, Schnetz-Boutaud N, Haines JL, Pericak-Vance MA (2009) CALHM1 polymorphism is not associated with late-onset Alzheimer disease. Ann Hum Genet 73:379–381. CrossRef Medline

Berridge MJ, Bootman MD, Lipp P (1998) Calcium—a life and death signal. Nature 395:645–648. CrossRef Medline

Bertram L, Schjeide BM, Hooli B, Mullin K, Hiltunen M, Soininen H, Ingelsson M, Lannfelt L, Blacker D, Tanzi RE (2008) No association between CALHM1 and Alzheimer's disease risk. Cell 135:993–994; author reply 994–996. CrossRef Medline

Bezprozvanny I, Mattson MP (2008) Neuronal calcium mishandling and the pathogenesis of Alzheimer's disease. Trends Neurosci 31:454–463. CrossRef Medline

Boada M, Antúnez C, López-Arrieta J, Galán JJ, Morón FJ, Hernández I, Marín J, Martínez-Lage P, Alegret M, Carrasco JM, Moreno C, Real LM, González-Pérez A, Tárraga L, Ruiz A (2010) CALHM1 P86L polymorphism is associated with late-onset Alzheimer's disease in a recessive model. J Alzheimers Dis 20:247–251. Medline

Bootman MD, Collins TJ, Mackenzie L, Roderick HL, Berridge MJ, Peppiatt CM (2002) 2-aminoethoxydiphenyl borate (2-APB) is a reliable blocker of store-operated Ca^{2+} entry but an inconsistent inhibitor of InsP3-induced Ca^{2+} release. FASEB J 16:1145–1150. CrossRef Medline

Boulay G, Zhu X, Peyton M, Jiang M, Hurst R, Stefani E, Birnbaumer L (1997) Cloning and expression of a novel mammalian homolog of *Drosophila* transient receptor potential (Trp) involved in calcium entry secondary to activation of receptors coupled by the Gq class of G protein. J Biol Chem 272:29672–29680. CrossRef Medline

Brenner S (1974) The genetics of *Caenorhabditis elegans*. Genetics 77:71–94. Medline

Carre-Pierrat M, Grisoni K, Gieseler K, Mariol MC, Martin E, Jospin M, Allard B, Ségalat L (2006) The SLO-1 BK channel of *Caenorhabditis elegans* is critical for muscle function and is involved in dystrophin-dependent muscle dystrophy. J Mol Biol 358:387–395. CrossRef Medline

Catterall WA (1993) Structure and function of voltage-gated ion channels. Trends Neurosci 16:500–506. CrossRef Medline

Chalfie M, Sulston JE, White JG, Southgate E, Thomson JN, Brenner S (1985) The neural circuit for touch sensitivity in *Caenorhabditis elegans*. J Neurosci 5:956–964. Medline

Chung S, Gumienny TL, Hengartner MO, Driscoll M (2000) A common set of engulfment genes mediates removal of both apoptotic and necrotic cell corpses in *C. elegans*. Nat Cell Biol 2:931–937. CrossRef Medline

Coe H, Michalak M (2009) Calcium binding chaperones of the endoplasmic reticulum. Gen Physiol Biophys 28:F96–F103. Medline

Dreses-Werringloer U, Lambert JC, Vingtdeux V, Zhao H, Vais H, Siebert A, Jain A, Koppel J, Rovelet-Lecrux A, Hannequin D, Pasquier F, Galimberti D, Scarpini E, Mann D, Lendon C, Campion D, Amouyel P, Davies P, Foskett JK, Campagne F, et al. (2008) A polymorphism in CALHM1 influences Ca^{2+} homeostasis, Abeta levels, and Alzheimer's disease risk. Cell 133:1149–1161. CrossRef Medline

Driscoll M, Chalfie M (1991) The *mec-4* gene is a member of a family of *Caenorhabditis elegans* genes that can mutate to induce neuronal degeneration. Nature 349:588–593. CrossRef Medline

Duerr JS, Frisby DL, Gaskin J, Duke A, Asermely K, Huddleston D, Eiden LE, Rand JB (1999) The *cat-1* gene of *Caenorhabditis elegans* encodes a vesicular monoamine transporter required for specific monoamine-dependent behaviors. J Neurosci 19:72–84. Medline

Etchberger JF, Hobert O (2008) Vector-free DNA constructs improve transgene expression in *C. elegans*. Nat Methods 5:3. CrossRef Medline

Fawcett GL, Santi CM, Butler A, Harris T, Covarrubias M, Salkoff L (2006) Mutant analysis of the Shal (Kv4) voltage-gated fast transient K+ channel in *Caenorhabditis elegans*. J Biol Chem 281:30725–30735. CrossRef Medline

Frøkjaer-Jensen C, Davis MW, Hopkins CE, Newman BJ, Thummel JM, Olesen SP, Grunnet M, Jorgensen EM (2008) Single-copy insertion of transgenes in *Caenorhabditis elegans*. Nat Genet 40:1375–1383. CrossRef Medline

Frøkjaer-Jensen C, Davis MW, Ailion M, Jorgensen EM (2012) Improved Mos1-mediated transgenesis in *C. elegans*. Nat Methods 9:117–118. CrossRef Medline

Gendrel M, Rapti G, Richmond JE, Bessereau JL (2009) A secreted complement-control-related protein ensures acetylcholine receptor clustering. Nature 461:992–996. CrossRef Medline

Gómez-Hernández JM, de Miguel M, Larrosa B, González D, Barrio LC (2003) Molecular basis of calcium regulation in connexin-32 hemichannels. Proc Natl Acad Sci U S A 100:16030–16035. CrossRef Medline

Hille B (2001) Ion channels of excitable membranes, Ed 3. Sunderland, MA: Sinauer.

Jan LY, Jan YN (1976) L-glutamate as an excitatory transmitter at the *Drosophila* larval neuromuscular junction. J Physiol 262:215–236. Medline

Jospin M, Jacquemond V, Mariol MC, Ségalat L, Allard B (2002) The L-type voltage-dependent Ca2+ channel EGL-19 controls body wall muscle function in *Caenorhabditis elegans*. J Cell Biol 159:337–348. CrossRef Medline

Karp SJ, Masu M, Eki T, Ozawa K, Nakanishi S (1993) Molecular cloning and chromosomal localization of the key subunit of the human N-methyl-D-aspartate receptor. J Biol Chem 268:3728–3733. Medline

Keramidas A, Moorhouse AJ, Schofield PR, Barry PH (2004) Ligand-gated

ion channels: mechanisms underlying ion selectivity. Prog Biophys Mol Biol 86:161–204. CrossRef Medline

Khakh BS, North RA (2006) P2X receptors as cell-surface ATP sensors in health and disease. Nature 442:527–532. CrossRef Medline

Kim H, Pierce-Shimomura JT, Oh HJ, Johnson BE, Goodman MB, McIntire SL (2009) The dystrophin complex controls BK channel localization and muscle activity in *Caenorhabditis elegans*. PLoS Genet 5:e1000780. CrossRef Medline

Krajacic P, Shen X, Purohit PK, Arratia P, Lamitina T (2012) Biomechanical profiling of *C. elegans* motility. Genetics 191:1015–1021. CrossRef Medline

Lambert JC, Sleegers K, González-PérezA, Ingelsson M, Beecham GW, Hiltunen M, Combarros O, Bullido MJ, Brouwers N, Bettens K, Berr C, Pasquier F, Richard F, Dekosky ST, Hannequin D, Haines JL, Tognoni G, Fiévet N, Dartigues JF, Tzourio C, et al. (2010) The CALHM1 P86L polymorphism is a genetic modifier of age at onset in Alzheimer's disease: a meta-analysis study. J Alzheimers Dis 22:247–255. Medline

Liu P, Ge Q, Chen B, Salkoff L, Kotlikoff MI, Wang ZW (2011a) Genetic dissection of ion currents underlying all-or-none action potentials in *C. elegans* body-wall muscle cells. J Physiol 589:101–117. CrossRef Medline

Liu P, Chen B, Wang ZW (2011b) Gap junctions synchronize action potentials and Ca2+ transients in *Caenorhabditis elegans* body wall muscle. J Biol Chem 286:44285–44293. CrossRef Medline

Liu Q, Chen B, Gaier E, Joshi J, Wang ZW (2006) Low conductance gap junctions mediate specific electrical coupling in body-wall muscle cells of *Caenorhabditis elegans*. J Biol Chem 281:7881–7889. CrossRef Medline

Lu B, Zhang Q, Wang H, Wang Y, Nakayama M, Ren D (2010) Extracellular calcium controls background current and neuronal excitability via an UNC79-UNC80-NALCN cation channel complex. Neuron 68:488–499. CrossRef Medline

Lytton J, Westlin M, Hanley MR (1991) Thapsigargin inhibits the sarcoplasmic or endoplasmic reticulum Ca-ATPase family of calcium pumps. J Biol Chem 266:17067–17071. Medline

Ma Z, Siebert AP, Cheung KH, Lee RJ, Johnson B, Cohen AS, Vingtdeux V, Marambaud P, Foskett JK (2012) CALHM1 is the pore-forming subunit of an ion channel that mediates extracellular Ca^{2+} regulation of neuronal excitability. Proc Natl Acad Sci U S A Plus 109:E1963–E1971. CrossRef Medline

MacDonald JF, Xiong ZG, Jackson MF (2006) Paradox of Ca^{2+} signaling, cell death and stroke. Trends Neurosci 29:75–81. CrossRef Medline

Maruyama T, Kanaji T, Nakade S, Kanno T, Mikoshiba K (1997) 2APB, 2-aminoethoxydiphenyl borate, a membrane-penetrable modulator of Ins(1,4,5)P3-induced Ca^{2+} release. Jpn J Biochem 122:498–505. CrossRef

Mayer ML, Westbrook GL, Guthrie PB (1984) Voltage-dependent block by Mg2+ of NMDA responses in spinal cord neurones. Nature 309:261–263. CrossRef Medline

Mello CC, Kramer JM, Stinchcomb D, Ambros V (1991) Efficient gene transfer in *C. elegans*: extrachromosomal maintenance and integration of transforming sequences. EMBO J 10:3959–3970. Medline

Minster RL, Demirci FY, DeKosky ST, Kamboh MI (2009) No association between CALHM1 variation and risk of Alzheimer disease. Hum Mutat 30:E566–E569. Medline

Morton E, Lamitina T (2010) A suite of MATLAB-based computational tools for automated analysis of COPAS Biosort data. Biotechniques 48:xxv–xxx. CrossRef Medline

Moyer BD, Hevezi P, Gao N, Lu M, Kalabat D, Soto H, Echeverri F, Laita B, Yeh SA, Zoller M, Zlotnik A (2009) Expression of genes encoding multitransmembrane proteins in specific primate taste cell populations. PLoS One 4:e7682. CrossRef Medline

Nowak L, Bregestovski P, Ascher P, Herbet A, Prochiantz A (1984) Magnesium gates glutamate-activated channels in mouse central neurones. Nature 307:462–465. CrossRef Medline

Richmond JE, Jorgensen EM (1999) One GABA and two acetylcholine receptors function at the *C. elegans* neuromuscular junction. Nat Neurosci 2:791–797. CrossRef Medline

Royal DC, Bianchi L, Royal MA, Lizzio M Jr, Mukherjee G, Nunez YO, Driscoll M (2005) Temperature-sensitive mutant of the *Caenorhabditis elegans* neurotoxic MEC-4(d) DEG/ENaC channel identifies a site required for trafficking or surface maintenance. J Biol Chem 280:41976–41986. CrossRef Medline

Rusakov DA, Fine A (2003) Extracellular Ca^{2+} depletion contributes to fast activity-dependent modulation of synaptic transmission in the brain. Neuron 37:287–297. CrossRef Medline

Saez JC, Berthoud VM, Branes MC, Martinez AD, Beyer EC (2003) Plasma membrane channels formed by connexins: their regulation and functions. Physiol Rev 83:1359–1400. Medline

Santi CM, Yuan A, Fawcett G, Wang ZW, Butler A, Nonet ML, Wei A, Rojas P, Salkoff L (2003) Dissection of K+ currents in *Caenorhabditis elegans* muscle cells by genetics and RNA interference. Proc Natl Acad Sci U S A 100:14391–14396. CrossRef Medline

Siebert AP, Ma Z, Grevet JD, Demuro A, Parker I, Foskett JK (2013) Convergent structural and functional evolution of CALHM ion channel with connexins and pannexins-innexins. J Biol Chem 288:6140–6153. CrossRef Medline

Smith SM, Bergsman JB, Harata NC, Scheller RH, Tsien RW (2004) Recordings from single neocortical nerve terminals reveal a nonselective cation channel activated by decreases in extracellular calcium. Neuron 41:243–256. CrossRef Medline

Syntichaki P, Xu K, Driscoll M, Tavernarakis N (2002) Specific aspartyl and calpain proteases are required for neurodegeneration in *C. elegans*. Nature 419:939–944. CrossRef Medline

Sznitman J, Purohit PK, Krajacic P, Lamitina T, Arratia PE (2010) Material properties of *Caenorhabditis elegans* swimming at low Reynolds number. Biophys J 98:617–626. CrossRef Medline

Taruno A, Vingtdeux V, Ohmoto M, Ma Z, Dvoryanchikov G, Li A, Adrien L, Zhao H, Leung S, Abernethy M, Koppel J, Davies P, Civan MM, Chaudhari N, Matsumoto I, Hellekant G, Tordoff MG, Marambaud P, Foskett JK (2013) CALHM1 ion channel mediates purinergic neurotransmission of sweet, bitter and umami tastes. Nature 495:223–226. CrossRef Medline

Tong YG, Bürglin TR (2010) Conditions for dye-filling of sensory neurons in *Caenorhabditis elegans*. J Neurosci Methods 188:58–61. CrossRef Medline

White MM, Aylwin M (1990) Niflumic and flufenamic acids are potent reversible blockers of Ca^{2+}-activated Cl-channels in Xenopus oocytes. Mol Pharmacol 37:720–724. Medline

Wu Y, Luo Y (2005) Transgenic *C. elegans* as a model in Alzheimer's research. Curr Alzheimer Res 2:37–45. CrossRef Medline

Xiong Z, Lu W, MacDonald JF (1997) Extracellular calcium sensed by a novel cation channel in hippocampal neurons. Proc Natl Acad Sci U S A 94:7012–7017. CrossRef Medline

Xu K, Tavernarakis N, Driscoll M (2001) Necrotic cell death in *C. elegans* requires the function of calreticulin and regulators of Ca^{2+} release from the endoplasmic reticulum. Neuron 31:957–971. CrossRef Medline

Xu W, Lipscombe D (2001) Neuronal Ca(V)1.3alpha(1) L-type channels activate at relatively hyperpolarized membrane potentials and are incompletely inhibited by dihydropyridines. J Neurosci 21:5944–5951. Medline

Zhang W, Bianchi L, Lee WH, Wang Y, Israel S, Driscoll M (2008) Intersubunit interactions between mutant DEG/ENaCs induce synthetic neurotoxicity. Cell Death Differ 15:1794–1803. CrossRef Medline